Reprinted from ENGINEERING FOR POWER, *Vol. 99, No. 3, July 1977*

K.P. Singh
President and CEO
Holtec International

A Method to Design Shell-Side Pressure Drop Constrained Tubular Heat Exchangers

In shell and tube heat exchangers, the triple segmental baffle arrangement has been infrequently used, even though the potential of this baffle system for high thermal effectiveness with low pressure drop is generally known. This neglect seems to stem from the lack of published design guidelines on the subject. Lately, however, with the rapid growth in the size of nuclear heat exchangers, the need to develop unconventional baffling pattern has become increasingly important. A method to effectively utilize the triple segmental concept to develop economical designs is presented herein. The solution technique given in this paper is based on a flow model named "Piecewise Continuous Cosine Model." The solution procedure easily lends itself to detailed analysis to determine safety against flow-induced vibrations.

1 Introduction

Large heat-transfer surface, often exceeding 10,000 sq ft, characterizes numerous auxiliary heat exchangers in conventional nuclear plants. Typical examples in such a category are the so-called Component Cooling Water Heat Exchangers, Shutdown Coolers, Residual Decay Heat Removal Heat Exchangers, etc. Considerations of pumping costs usually restrict the permissible pressure drop in the shell side stream to rather low values (typically 10–15 psi). This restriction may sometimes become a major impediment in an efficient design. The most convenient palliative is to prescribe a large shell diameter to make the tube bundle short and "stubby" and thus reduce the crossflow velocity and travel path of the shell stream. However, such a solution is intrinsically expensive, since the shell diameter has a direct bearing on the equipment cost. A preferable solution is to devise an appropriate baffling pattern that possesses an inherent ability to produce low pressure drops combined with efficient heat transfer.

Another important design consideration is the structural integrity of the tube bundle. The occurrence of flow-induced tube vibration in nuclear heat exchangers has become menacingly frequent enough to warrant close attention at the design stage [1].[1] The main flow variable responsible for inducing tube resonance in liquid-to-liquid heat exchange equipment is the crossflow velocity; defined as the component of shell stream velocity vector perpendicular to the tube axis. Hence, any effort to reduce the crossflow velocity in critical regions would aid in mitigating the possibility of tube vibration.

Thus the quest for a suitable baffling poses two primary requirements on the baffle, namely (1) an ability to produce low pressure drop and (2) a built-in flexibility to reduce crossflow in regions of low tube frequency (window tube spans). A promising concept embodying the aforementioned attributes is the so-called Triple Segmental Baffle Layout (TSBL), shown in Fig. 1. The triple segmental baffle assembly consists of three distinct baffle types (Fig. 3), which we designate as the solid baffle (Fig. 3(*a*)), single slot baffle (Fig. 3(*c*)), and double slot baffle (Fig. 3(*b*)). These baffles are arranged at a suitable uniform spacing, as shown in Fig. 2. It becomes readily apparent that the triple segmental baffle is a natural extension of the well-known segmental [2], and not so well-known double segmental design.[2] The heat transfer and hydraulic characteristics of segmental baffles have been correlated by numerous researchers [4]. The most recent of the major efforts on this subject was made by the investigators at the Heat Transfer Research Institute (HTRI) [7], who developed the Stream Analysis Method based on Tinker's model [5, 6]. Stream Analysis Method has become a popular solution technique, and the computer programs based on this method have acquired widespread acceptance, even though the researches of HTRI are proprietary to its member companies, and hence inaccessible to an important segment of the academe. The Stream Analysis Method was recently extended by HTRI to double segmental baffles in a rather rudimentary form. The lack of sufficient experimental data has hampered the development

[1] Numbers in brackets designate References at end of paper.

Contributed by the Power Division and presented at the Joint Power Generation Conference, Buffalo, N. Y., September 19–22, of THE AMERICAN SOCIETY OF MECHANICAL ENGINEERS. Manuscript received at ASME Headquarters June 16, 1976. Paper No. 76-JPGC-NE-1.

[2] Referred to as "strip" type by Mueller [3].

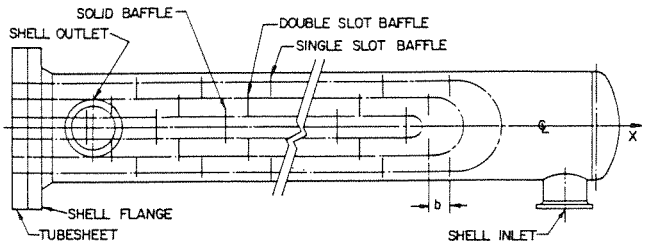

Fig. 1 Triple segmental baffle layout

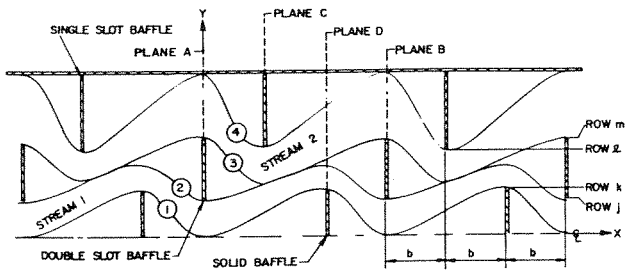

Fig. 2 Piecewise Continuous Cosine Model

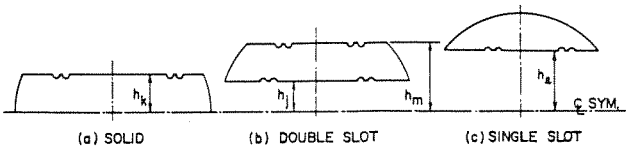

Fig. 3 Baffle geometries

of a Stream Analysis Method for the double segmental baffles that is equal in sophistication to the single segmental type. The situation is even worse for the triple segmental geometry. To the best of our knowledge, the experimental studies on pressure drop and heat transfer characteristics of triple segmental baffled bundles are nonexistent in the open literature. This has inhibited the development of proper design guidelines for TSBL and hence its use in the industry.

In this paper we present a rational design method for TSBL, based on the well-known correlations for flow across and parallel to ideal tube banks. The main theme of this paper is in the development of Stream Allocation Technique (SAT) using a Piecewise Continuous Cosine Model. The concept of SAT is described in Section 3. The range of applicability of the method proposed herein will remain limited until sufficient experimental data are generated and utilized to introduce the empirical constants that are necessary where idealized solutions are applied to a broad range of conditions in practical equipment.

The method proposed here has been developed over the last five years and used to design a number of heat exchangers for several nuclear plants. Unfortunately, many of the performance data are not yet available, since most of the plants are not yet operational. However, it is hoped that this solution will stimulate interest among experimentalists to improve upon the correlations given this paper.

It is important to point out the range of applicability of the solution proposed in this work. The main limitations are:

1 Size: Small diameter shells (under 30 in., typically) are excluded. The triple segmental arrangement is not suitable for tube bundles with fewer than 30 tube rows.

2 Bare tubes: The effect of improved heat transfer by the use of fins and other turbulence promotion devices is not considered in this paper. This method can, however, be extended to eliminate this restriction.

3 Fabrication: The fabrication methods and tolerances are assumed to be in accordance with Tema [19].

4 Flow medium: The shell side medium is assumed to be liquid.

5 Pitch: The tube layout pitch is assumed to be uniform.

6 Impingement plates: It is assumed that the tube bundle contour is roughly circular, i.e., impingement plates are not present. The impingement plates introduce void areas in the shell and asymmetry in the bundle profile [20], which are not accounted for in the present analysis.

Quantitatively speaking, TSBL merits consideration for heat exchangers over 30 in. in diameter and becomes an increasingly attractive design for larger shells.

An alternate concept for pressure drop constrained designs is the so-called no-tubes-in-window construction. The no-tubes-in-window geometry is a variant of the classical segmental baffle design in which the tubes are removed from the window region. Thus the window velocity and crossflow path between the baffle tips are reduced. All tubes are supported at each baffle, thereby improving the ability of the tubes to withstand higher shell crossflow velocities than could be admissible in the conventional designs. However, sometimes the

Nomenclature

a_i = amplitude of Streamline i
A_F = total flow area at a generic point 0 (Fig. 4)
A_0 = open longitudinal flow area
b = baffle spacing
d_0 = outside diameter of tube
D' = equivalent hydraulic diameter (equation 42)
f_c = isothermal friction factor
f_e = in-tube friction factor
g = gravitational constant
h_{ij} = crossflow coefficient of Stream i in compartment j
h_i = height of row i
h_c = crossflow film coefficient
h_l = longitudinal film coefficient
h_s = shell side film coefficient
k = thermal conductivity of shell side fluid
M = total number of tube rows in each half of shell
N = total number of tubes
N_1 = number of tubes in the region of Steam 1
N_e = number of tube rows crossed (equation 20)
Nu = Nusselt number
P_e = longitudinal pitch
P_0 = wetted perimeter
Pr = Prandtl number
Q = overall heat duty
R = bundle outer radius
Re = Reynolds number
r_i = offset of Streamline i (i = 1, 4)
U_{ij}' = window velocity of Stream i at threshold to compartment j (i, j = 1, 2)
V_{ij} = crossflow velocity of Stream i in compartment j (i, j = 1, 2)
W_{ij} = flow velocity of Stream i, compartment j (i, j = 1, 2)
W^i = total flow in Stream i (i = 1, 2)
$W_H{}^i$ = total flow for heat transfer in Stream i (i = 1, 2)
$y_{k'}$ = height (y-coordinate) of central overlap row for Stream 1
$y_{l'}$ = height (y-coordinate) of central overlap row for Stream 2
ΔP = shell side pressure drop for one baffle set
η_c = effectiveness coefficient for crossflow stream
η_l = effectiveness coefficient for longitudinal stream
κ = Effective stream fraction multiplier (equation 18)
μ_w, μ_b = shell liquid viscosity at wall and bulk temperature, respectively
ρ = density of shell side liquid at bulk temperature
ω_{ij} = lost velocity vector in turnaround at threshold to compartment j in Stream i
Ω = total flow area
$\Omega_A, \Omega_B, \Omega_C, \Omega_E, \Omega_F$ = total flow area for substreams A, B, C, E, and F, respectively

baffles may have to be placed quite far apart to meet the pressure drop restrictions, in which case intermediate support plates between the baffles may be required. A major drawback in the no-tubes-in-window design is the increase in shell diameter due to removal of tubes from the window. In high-pressure applications (design pressure in excess of 250 psi), the heat exchanger cost rises steeply with the shell diameter, which may render the no-tubes-in-window design uneconomical. This drawback is partially mitigated where impingement plates are required at the shell inlet.

To date, little research effort has been directed toward studying the special nuances of the no-tubes-in-window design, e.g., influence of the intermediate support plates, wide baffle spacings, etc. Nevertheless, the no-tubes-in-window concept has been gaining acceptance in the industry. The heat exchanger designer should consider its use in pressure drop restricted designs.

In this paper, however, we will confine our treatment to the triple segmental baffle layout (TSBL). The method given in this paper may be used to determine the overall pressure drop and shell side film coefficient for a given tube and baffle layout. The details of the exchanger rating technique are omitted here, since they are well documented in the literature.

2 Piecewise Continuous Cosine Streamline Model

The triple segmental baffle layout (TSBL) consists of three distinct baffle types (Fig. 2) laid out alternately at a uniform spacing b, as shown in Fig. 2. Let us assume that each half of the shell contains M tube rows. Let n_i denote the number of tubes in row i, thus

$$N = 2\sum_{i=1}^{M} n_i \tag{1}$$

The baffle cuts are determined such that the net window flow velocity at each baffle is as nearly equal as possible. The tube row overlap is set equal to the minimum admissible, which is two tube rows (one complete tube row common to both baffles). The overlap may be increased where final calculations indicate that additional pressure drop in the shell side is available. This is discussed further in Section 6.

Let tube rows j, k, l, and m denote the locations (row number) of baffle cuts (Fig. 3), and h_i denote the perpendicular distance of plane of row i (xz plane) from the center line. Furthermore, let

$$h_j' = 0.5(h_j + h_m) \tag{2}$$

Fig. 2 shows that the shell flow can be idealized as consisting of four streams, two in each half of the shell. The two distinct streams are labeled as Stream 1 and Stream 2. Both streams have a doubly periodic profile due to the geometry of baffle arrangement. The harmonic pattern of the streams suggests a method for mathematical quantification, which we term Piecewise Continuous Cosine Model.

It is recognized that the shell flow in the turbulent range is highly statistical in nature consisting of random material derivatives of velocity. However, in practical designs one is concerned only with evaluating the gross integrated effects, e.g., heat transfer, pressure loss, etc. An idealized stream model may be constructed to predict the gross effects, provided the inherent limitations of such models in regard to their range of applicability is properly understood.

The Piecewise Continuous Cosine Model envisages each stream defined by two bounding streamlines. Thus Stream 2 is bounded by Streamlines 3 and 4. Similarly Stream 1 is bounded by Streamlines 1 and 2. Each streamline is represented by two cosine curves in a set of baffles. Thus Streamline 4 bounding Stream 2 from above (Fig. 2) can be represented by

$$y_4 = r_4 + a_4 \cos\frac{\Pi x}{b}; \qquad 0 \le x \le b$$

$$= r_r - a_4 \cos\frac{\Pi(x-b)}{2b}; \qquad b \le x \le 3b \tag{3}$$

where

$$r_4 = 0.5(h_M + h_l)$$

and

$$a_4 = 0.5(h_M - h_l) \tag{4}$$

Similarly, the equation for Streamline 1 bounding Stream 1 from below (Fig. 2) can be written by direct inspection

$$y_1 = r_1 - a_1 \cos\frac{\Pi x}{2b}; \qquad 0 \le x \le 2b$$

$$= r_1 + a_1 \cos\frac{\Pi(x-2b)}{b}; \qquad 2b \le x \le 3b \tag{5}$$

where

$$r_1 = a_1 = 0.5h_k \tag{6}$$

In a similar manner, the equations for Streamlines 2 and 3 can be written

$$y_3 = r_3 + a_3 \cos\frac{\Pi x}{b}; \qquad 0 \le x \le b \tag{7a}$$

$$= r_3 - a_3 \cos\frac{\Pi(x-b)}{2b}; \qquad b \le x \le 3b \tag{7b}$$

$$y_2 = r_2 - a_2 \cos\frac{\Pi x}{2b}; \qquad 0 \le x \le 2b \tag{8a}$$

$$= r_2 + a_2 \cos\frac{\Pi(x-2b)}{b}; \qquad 2b \le x \le 3b \tag{8b}$$

To determine the offset r_i and amplitude a_i ($i = 2, 3$) of "interface streamlines" (Streamlines 2 and 3), we assume that the two streamlines contact at $y = h_{j'}$ where $h_{j'}$ is defined by equation (2). Let $x = x^*$ at the point of contact, then from equation (7b), we have

$$h_{j'}, r_3 - a_3 \sin\frac{\Pi x^*}{2b} \tag{9}$$

Similarly equation (8a) yields

$$h_{j'} = r_2 - a_2 \cos\frac{\Pi x^*}{2b} \tag{10}$$

Finally, the point of contact implies

$$\frac{dy_2}{dx} = \frac{dy_3}{dx}\bigg|_{x=x^*} \tag{11}$$

Equation (11) in conjunction with equations (7) and (8) yields

$$\tan\frac{\Pi x^*}{2b} = \frac{-a_3}{a_2} \tag{12}$$

Furthermore, we note

$$r_3 + a_3 = h_m \tag{13}$$

$$r_2 - a_2 = h_j \tag{14}$$

It can be shown, after some algebra, using equations (9)–(14), that

$$\frac{h_m - h_{j'}}{h_{j'} - h_j} = -\tan\frac{\Pi x^*}{2b}\,\frac{1 + \sin\dfrac{\Pi x^*}{2b}}{1 - \cos\dfrac{\Pi x^*}{2b}} \tag{15}$$

Substituting for $h_{j'}$ from equation (2) in equation (15), and solving for x^* yields $x^* = 1.5b$.

Having determined x^*, equations (9) and (13) yield r_3 and a_3. Similarly equations (10) and (14) yield r_2 and a_2.

Finally, it is convenient to define the mean surface of each stream, given by the mean curve of the two bounding streamlines in the xy plane. Thus, the mean streamlines for Streams 1 and 2 are defined by

$$y' = 0.5(y_1 + y_2); \quad \text{for Stream 1}$$

$$y'' = 0.5(y_3 + y_4); \quad \text{for Stream 2} \tag{16}$$

where y_i ($i = 1, 4$) are defined in the preceding paragraphs. It is also contextual to define the "central overlap row" for each stream. Referring to Fig. 1, the y coordinate of the central overlap row for the two streams is given by

$$y_{k'} = 0.5(h_j + h_k); \quad \text{for Stream 1}$$
$$y_{l'} = 0.5(h_l + h_m); \quad \text{for Stream 2} \tag{17}$$

Equations (3)–(17) define major geometry variables that define the Piecewise Continuous Cosine Streamline Model proposed in this work. It is to be emphasized that this model is merely an artifice to predict the gross effects of highly indeterminate structure of turbulent flows. Further improvements in the predictions will undoubtedly follow from experimental data.

It is of some importance to observe that this model exhibits the main strength of the triple segmental design; namely (1) reduced shell crossflow velocity resulting in increased protection against flow-induced vibration, (2) short crossflow path reducing crossflow pressure drop, (3) increased window areas (over segmental or strip designs), which minimize window turnaround and friction loss.

Having thus prescribed the stream profiles, it is now possible to determine their ratio by equating the pressure drops between plane A and plane B in Fig. 1. An additional complication is introduced due to the so-called leakage and bypass substreams [7]. These substreams may become significant in some designs and may strongly influence the exchanger performance [9]. A brief qualitative description of the various substreams is given here to place their importance in proper perspective.

Following Tinker [6] and Taborek [9], the shell stream may be subdivided into five component substreams as described here:

A Substream: Flow through the clearance between the tube and baffle holes. This component would be small for baffles drilled with extra tight clearances (typically 0.04 mm on diameter), and in designs involving small crossflow pressure drops, e.g., the TSBL designs. *A* Substream is considered effective in heat transfer.

B Substream: This is the true crossflow stream; it should be over 80 percent of the total in well designed units.

C Substream: The stream between the bundle and the shell; it follows a helical path around the bundle. Sealing strips, dummy tubes, etc., may be used to minimize this stream. This stream is only partially effective in heat transfer.

E Substream: This is the baffle-to-shell leakage stream. This is the most inefficient component of flow. In addition to being ineffective in heat transfer, it may distort the temperature profile resulting in reduced LMTD. This is discussed in depth in reference [9].

F Substream: This is the substream through the pass partition gaps located in the xy plane. This component, like *C* Substream, is only partially effective in heat transfer, and can be reduced by use of dummy tubes.

Determination of the proportions of the aforementioned substreams is difficult, principally because the flow path resistances for each component are difficult to establish. The HTRI investigators developed semitheoretical models for flow path resistances, which needed to be modified by correlation with experimental data. Since no experimental data for triple segmental designs exist, it is premature at this time to seek the true substream ratios. Instead we propose simple flow proportions, which give conservative results for most designs. Possible theoretical basis to determine the true stream resistances to apply the Stream Analysis Method to the triple segmental design is presently being developed by the authors.

For simplicity it is proposed here to apportion the substreams in the ratio of the flow area available for each one of them. For Substream *A*, the flow area Ω_A is the net clearance area between the tube and baffle holes in the baffle overlap region. For Substream *B*, the flow area Ω_B is taken as the nominal crossflow area between the extreme tubes at the central overlap row defined by equation (17). Similarly, the flow area for Substream *C*, Ω_C, is the nominal end zone gap area in the vicinity of the central overlap row. The flow areas for Substreams *E* and *F* are similarly calculated.

It is recognized that the aforementioned assumption will in general underpredict the *B* component and overpredict the others. The danger of error on the unsafe side is obviated by using only the *B* substream in heat transfer calculations, and treating it as though the entire stream is in crossflow in computing the pressure loss.

Thus if W^1 be the total flow in Stream 1, then the crossflow stream for heat transfer calculations $W_H{}^1$ is given by

$$W_H{}^1 = \frac{\Omega_B}{\Omega} W^1 = \kappa W^1 \tag{18}$$

where

$$\Omega = \Omega_A + \Omega_B + \Omega_C + \Omega_E + \Omega_F \tag{19}$$

and κ is defined as the effective stream fraction multiplier.

If the flow path resistances for each stream are established, then an iterative solution akin to the Stream Analysis Method of Palen and Taborek [7] can be developed to determine the substream quantities. Research in this area will yield substantive improvement in accuracy of the results predicted by the method proposed in this work.

We next describe the method to determine the pressure drop and stream fraction, W^1/W^2.

3 Stream Allocation Technique

To determine the ratio of flow rates in Streams 1 and 2, the pressure drop between planes *A* and *B* in the two streams is equated (Fig. 2). To fix ideas, we subdivide the span between planes *A* and *B* into two compartments. For Stream 1, compartments 1 and 2 are defined by the regions between planes *A* and *D*, and planes *D* and *B*, respectively. For Stream 2, compartments 1 and 2 are defined by the regions between planes *A* and *C*, and planes *C* and *B*, respectively. The general notation for the crossflow velocity in compartment j ($j = 1, 2$) of stream i ($i = 1, 2$) is V_{ij}. Similarly U_{ij}' denotes the window velocity at the threshold of compartment j in stream i. For example, U_{11}' denotes window velocity at plane *A* in Stream 1. W_{ij} denotes the total velocity vector for stream i and compartment j.

It is intuitively obvious that Stream 2 will have a longer flow path and smaller crossflow area than Stream 1, and hence it will be generally smaller in magnitude than Stream 1. However, we will assume the two streams to be equal to start an iteration process. We will develop expressions for the total pressure drop ΔP in one complete set of baffles (between planes *A* and *B* in Fig. 2) for Stream 1. The equivalent expressions for Stream 2 can be constructed by direct analogy.

The total pressure drop ΔP consists of six major components; namely (1) crossflow friction loss in compartment 1, ΔP_{11}; (2) crossflow friction loss in compartment 2, ΔP_{12}; (3) window turnaround loss at the threshold to compartment 1, ΔP_{13}; (4) window turnaround loss at the threshold to compartment 2, ΔP_{14}; (5) longitudinal friction loss in compartment 1, ΔP_{15}; (6) longitudinal friction loss in compartment 2, ΔP_{16}.

Equations to determine each of the foregoing pressure drop components are given in the following:

1 Crossflow Friction Loss in Compartment 1. Following the analogy of ideal tube banks, the crossflow pressure drop is given by

$$\Delta P_{11} = 4 f_c \left(\frac{\rho V_{11}{}^2}{2g}\right) N_e \left(\frac{\mu_w}{\mu_b}\right)^{0.14} \tag{20}$$

where μ_w and μ_b are wall and bulk temperature dynamic viscosities of the fluid, respectively; ρ is fluid density, g is gravitational constant, N_e is the number of tube rows crossed, f_c is isothermal friction factor, and V_{11} is the crossflow velocity.

The isothermal friction factor f_c has been measured be several investigators [10, 11]. According to Žukauskas [12], f_c approaches a constant value in the supercritical range for a given layout pattern. In the subcritical turbulent region, f_c can be represented as a power function of the Reynolds number Re, i.e.:

$$f_c = \frac{c'}{\mathrm{Re}^n} \tag{21}$$

where c' and n are functions of the transverse pitch, longitudinal pitch, and pitch to diameter ratio. Typically, $f_c < 0.1$ for Re = 10,000

and <0.05 for Re $\simeq 10^6$ for 45 deg layout. For 30 deg layout, $f_c < 0.13$ for Re = 10,000, and <0.05 for Re $\simeq 10^6$.

The effective number of tube rows crossed is given by the average number of tube rows traversed by Streamlines 1 and 2, i.e., by twice the amplitude of the mean streamline. Thus

$$N_e = \frac{1}{P_e}[a_1 + a_2] \tag{22}$$

where P_e is longitudinal pitch (spacing between tube rows).

The crossflow velocity V_{11}, however, varies as the stream traverses its crosspath. To determine the crossflow velocity as a function of y, we consider the mean line (equation (16)). The equation of the mean line for Stream 1 follows from equations (5), (8), and (16):

$$y' = r_{12} - a_{12}\cos\frac{\Pi x}{2b}; \qquad 0 \le x \le 2b$$
$$y' = r_{12} + a_{12}\cos\frac{\Pi(x-2b)}{b}; \qquad 2b \le x \le 3b \tag{23}$$

where

$$r_{12} = (r_1 + r_2)/2$$
$$a_{12} = (a_1 + a_2)/2 \tag{24}$$

The flow profile at any location will be established by the mean streamline. The slope of the streamline at a generic point 0 (x_0, y_0) (see Fig. 4) is given by

$$\tan\phi = \frac{\Pi}{2b}a_{12}\sin\frac{\Pi x_0}{2b}; \qquad x \le 2b \tag{24a}$$
$$= -\frac{\Pi}{b}a_{12}\sin\frac{\Pi(x_0-2b)}{b}; \qquad b \le x \le 3b \tag{25b}$$

Hence, the equation of line A_1A_2 (perpendicular to the flow front at point 0) is given by

$$(x - x_0) = -\tan\phi\,(y - y_0) \tag{26}$$

Equation (26) in conjunction with the equation for Streamlines 1 and 2 (equations (5) and (8)) must be solved to determine the coordinates for points A_1 and A_2, respectively. It can be shown that x_1 and x_2 are given by

$$a_i\cos\frac{\Pi x_i}{2b} + y_0 - r_i + (x_0 - x_i)\cot\phi = 0; \qquad x \le 2b \tag{27a}$$
$$a_i\cos\frac{\Pi(x_i-2b)}{b} - y_0 + r_i - (x_0 - x_i)\cot\phi = 0; \qquad 2b \le x \le 3b \tag{27b}$$
$$i = 1, 2$$

where ϕ is defined by equation (25). Equations (27) must be solved by a trial and error method, such as Newton-Raphson [15, p. 319]. The total flow area A_F is given by

$$A_F = \frac{R}{\cos\phi}\left\{\left[y_2\cos\left(\sin^{-1}\frac{y_2}{R}\right) - y_1\cos\left(\sin^{-1}\frac{y_1}{R}\right)\right] + R^2\left(\sin^{-1}\frac{y_2}{R} - \sin^{-1}\frac{y_1}{R}\right) - \frac{\Pi d_0^2}{4}\sum_{i=i^*}^{j^*} n_i\right\} \tag{28}$$

where i^* and j^* are defined by the following inequalities:

$$h_{i^*} > y_1 > h_{i^*-1}$$
$$h_{j^*+1} > y_2 > h_{j^*} \tag{29}$$

The gross velocity W_{11} at 0 is given by dividing the flow rate W_{11} by A_F. The cross flow component V_{11} is given by

$$V_{11} = W_{11}\sin\phi \tag{30}$$

Let V_{11i} denote the crossflow velocity at the ith traversed row; then the equation for the crossflow pressure drop may be written as

$$\Delta P_{11} = 4\frac{\rho}{2g}\left(\frac{\mu_w}{\mu b}\right)^{0.14}\sum_{i=1}^{N_e} f_c V_{11i}^2 \tag{31}$$

Substituting for f_c from equation (21), we have

$$\Delta P_{11} = \Lambda'\sum_{i=1}^{N_e} V_{11i}^{(2-n)} \tag{32}$$

where Λ' is defined by

$$\Lambda' = \frac{4c'}{\left(\frac{\rho d}{\mu}\right)^n}\frac{\rho}{2g}\left(\frac{\mu_w}{\mu_b}\right)^{0.14} \tag{33}$$

2 Crossflow Friction Loss in Compartment 2. The calculation procedure is identical to that described in the preceding paragraphs. Equations (25*b*), (26), (27*b*), and (28) determine A_F.

3 Window Turnaround Loss at Threshold to Compartment 1. The cosine streamline model developed in this paper yields a continuously varying flow velocity vector which is parallel to the x-axis at the window locations and reaches a maximum slope of $\Pi/4$ rad at middistance in each compartment. An approximate expression for the kinetic energy loss may be found by assuming the mean cross velocity vector to be directed along the points of intersection of the mean streamline at contiguous windows.

From equation (5), (8), and (16), it can be shown that the equation of the mean streamline is given by

$$y' = \frac{1}{2}\left[r_1 - a_1\cos\frac{\Pi x}{2b} + r_2 - a_2\cos\frac{\Pi x}{2b}\right]; \qquad 0 \le x \le 2b$$
$$y' = \frac{1}{2}\left[r_1 + a_1\cos\frac{\Pi(x-2b)}{b} + r_2 + a_2\cos\frac{\Pi(x-2b)}{b}\right]; \qquad 2b \le x \le 3b \tag{34}$$

From equations (34), the assumed angle of approach of the flow velocity vector W_{12} at $x = 0$ is given by

$$\theta_{12} = \tan^{-1}\frac{a_1 + a_2}{b} \tag{35}$$

Similarly, the angle of approach θ_{11} at $x = 2b$ (plane D) is

$$\theta_{11} = \tan^{-1}\frac{a_1 + a_2}{2b} \tag{36}$$

The vector equilibrium of the velocities is shown in Fig. 5. If it is conservatively assumed that the make-up velocity vectors ω_{12} and ω_{11} are irretrievably lost in the window turnaround at plane A, then the total pressure drop due to turnaround is

$$\Delta P_{13} = \frac{\rho}{2g}(\omega_{11}^2 + \omega_{12}^2) \tag{37}$$

where

$$\omega_{11}^2 = U_{11}'^2 + W_{11}^2 - 2U_{11}'W_{11}\cos\theta_{11} \tag{38}$$
$$\omega_{12}^2 = U_{11}'^2 + W_{12}^2 - 2U_{11}'W_{12}\cos\theta_{12} \tag{39}$$

where W_{11} is the flow velocity vector evaluated at $x = b$; and W_{12} is the flow velocity vector at $x = 2.5b$. U_{11}' is the flow velocity at the threshold to compartment 1, i.e., at plane A.

4 Window Turnaround Loss at Threshold to Compartment 2. The pressure loss ΔP_{14} is given by equation (37), where U_{12}' replaces U_{11}' in the definitions of ω_{11} and ω_{12} (equations (38) and (39)).

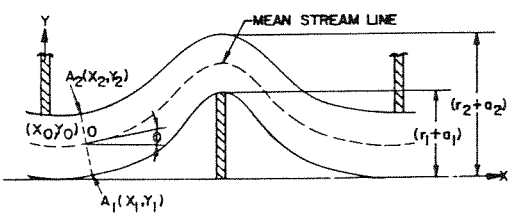

Fig. 4 Typical stream profile

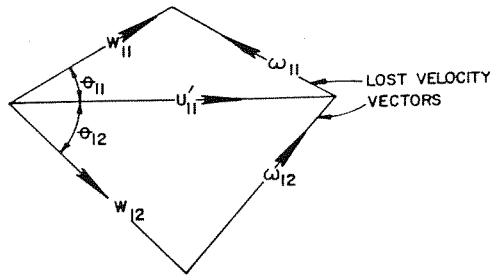

Fig. 5 Vectorial equilibrium of velocities at plane *A* (stream 1)

5 Longitudinal Friction Loss in Compartment 1. The longitudinal component of pressure drop may be a significant portion of the total because of the predominant longitudinal component of the flow velocity vector. Using the well-known Fanning formulation, the pressure drop in the span of compartment 1 may be given by

$$\Delta P_{14} = \frac{\rho}{2g}\int_0^{2b} \frac{4f_e}{D'} u^2 dx \tag{40}$$

where f_e is in-tube friction factor and u is the longitudinal component of the flow velocity. Experimentally measured and correlated values of f_e appear in various publications [13, 14]. f_e can be expressed as a power function of the Reynolds number Re′ in the subcritical range [8, p. 266].

$$f_e = \frac{0.08}{\mathrm{Re}'^{1/4}} \tag{41}$$

Where Re′ is Reynolds number for longitudinal flow. f_e given by equation (41) is valid for $\mathrm{Re}' < 2 \times 10^5$ in the turbulent range, which covers the normal range encounted in tubular heat exchangers. The Reynolds number Re′ is based on the equivalent hydraulic diameter D' of the flow regime. The hydraulic diameter D' is defined as

$$D' = \frac{4 \times \text{open longitudinal flow area}}{\text{total wetted perimeter}} \tag{42}$$

Due to the nature of the flow regime, the open longitudinal flow area A_0 and wetted perimeter P_0 are functions of x. For Stream 1, it can be readily shown that

$$A_0 = R\left(y_2 \cos \sin^{-1}\frac{y_2}{R} - y_1 \cos^{-1} \sin \frac{y_1}{R} + R^2\left(\sin^{-1}\frac{y_2}{R} - \sin^{-1}\frac{y_1}{R}\right) - \frac{\Pi {d_0}^2}{4} N^* \right. \tag{43}$$

where y_2 and y_1 are defined by equations (8) and (5), respectively, and

$$N^* = \sum_{i^*}^{j^*} n_i \tag{44}$$

where i^* and j^* are defined by

$$h_{i^*} > y_1 > h_{i^*-1} \tag{45a}$$

$$h_{j^*+1} > y_2 > h_{j^*} \tag{45b}$$

Similarly, the wetter perimeter P_0 is given by

$$P_0 = \Pi d_0 N^* + R\left(\sin^{-1}\frac{y_2}{R} - \sin^{-1}\frac{y_1}{R}\right) \tag{46}$$

Substituting for f_e from equation (41) in equation (40), yields

$$\Delta P_{14} = \frac{2\rho}{g}\int_0^{2b} \frac{-0.08u^2}{\mathrm{Re}^{1/4} D'} dx \tag{47}$$

where

$$\mathrm{Re}' = \frac{\rho u D'}{\mu} \tag{47a}$$

Substituting for Re′ in equation (47) yields

$$\Delta P_{14} = \frac{0.16\rho^{0.75}\mu^{0.25}}{g}\int_0^{2b} \frac{u^{1.75}}{D'^{1.25}} dx \tag{48}$$

where the longitudinal flow velocity u at a generic point 0 (Fig. 4) is given by

$$u = W_{ij} \cos \phi \tag{49}$$

where W_{ij} is the flow velocity (in Stream i, compartment j) based on A_F (equation (28)). The integration in equation (48) is performed using a numerical quadrature scheme, such a Simpson's rule [15].

6 Longitudinal Friction Loss in Compartment 2. ΔP_{16}. This component can be calculated in the same manner as ΔP_{15}. The appropriate expression for the longitudinal flow velocity should be derived using the applicable streamline equations. Detailed derivation is omitted for brevity.

Thus the total pressure drop in one set of baffles for Stream 1 is given by

$$\Delta P_1 = \Delta P_{11} + \Delta P_{12} + \Delta P_{13} + \Delta P_{14} + \Delta P_{15} + \Delta P_{16} \tag{50}$$

where ΔP_{1i}, $i = 1, 2, \ldots 6$ are defined in the preceding paragraphs.

In a similar manner, the total pressure drop for Stream 2 between planes A and B can be computed.

To start an iteration process, the two streams are assumed to be equal in magnitude. Then the pressure drops ΔP_1 and ΔP_2 in the two strems are calculated. If ΔP_1 and ΔP_2 are not equal (within a practical tolerance) then W^1 and W^2 are readjusted, and the procedure is continued. The following iteration scheme yielded fast convergence. At iteration No. i, the flow rate in Stream 1 was adjusted to $W_i{}^1$ where

$$W_i{}^1 = W_{i-1}{}^1\left[1 - \frac{1}{\Lambda}\left\{1 - \left(\frac{\Delta P_1{}^{i-1}}{\Delta P_2{}^{i-1}}\right)^{1/2}\right\}\right] \tag{50a}$$

where $\Delta P_j{}^{i-1}$ is the pressure drop in stream j at iteration No. $i-1$ and Λ is a sensitivity constant. Convergence (defined by $|(\Delta P_1 - \Delta P_2)/\Delta P_2| \leq 0.005$) was obtained in 3 to 4 iterations by setting $\Lambda =$ 4 or 5.

4 Shell Side Film Coefficient

The shell side film coefficient consists of two components, namely (*a*) the crossflow coefficient h_c, and (*b*) the longitudinal flow coefficient, h_l. The longitudinal component of total pressure drop is significant in TSBL, and hence its contribution in heat transfer cannot be ignored. Equations to determine h_c and h_l are constructed in the following:

(*a*) Crossflow Film Coefficient: h_c. We utilize the well-known correlation for the so-called ideal tube banks to estimate h_c.

$$\frac{h_c d_0}{k} = 0.38\ \mathrm{Re}^{0.6}\mathrm{Pr}^{1/3} \tag{51}$$

In equation (51) k denotes thermal conductivity of the fluid, and Pr denotes the Prandtl number referred to the mean bulk temperature of the fluid. The Reynolds number Re depends on the crossflow velocity V_{ij}, and the effective stream fraction multiplier (equation (18)); i.e.,

$$\mathrm{Re} = \frac{\rho\kappa V_{ij} d_0}{\mu} \tag{52}$$

V_{ij} is calculated in the manner described in Section 3 (equation (30)). κ is introduced in the definition of the Reynolds number (equation (52)) for conservatism, as discussed in Section 3. Thus for the ith traversed row in Stream 1, the local crossflow film coefficient is

$$h_{ci} = \chi_c v_{11i}$$

where

$$\chi_c = \frac{0.38k}{{d_0}^{0.4}}\left(\frac{\kappa\rho}{\mu}\right)^{0.6}\mathrm{Pr}^{1/3} \tag{54}$$

Thus the average crossflow film coefficient for Stream 1 (compart-

ment 1) is given by

$$h_c = \chi_c \frac{1}{N_e} \sum_{i-1}^{N_e} V_{11i}{}^{0.6} \tag{54}$$

(b) Longitudinal Film Coefficient: h_l. The longitudinal film coefficient is related to the longitudinal flow Reynolds number Re′ by the well-established correlation for flow in pipes [4, p. 158]:

$$\text{Nu} = 0.023\ \text{Re}'^{0.8}\ \text{Pr}^{1/3} \tag{55}$$

where Nu and Pr denote Nusselt and Prandtl numbers, respectively. Re′ is defined by equation (47a). Introducing the effective stream fraction multiplier κ in the definition of the Reynolds number Re′, the local film coefficient at a generic point 0 is given by

$$h_l' = 0.023\ \text{k} \left(\frac{\kappa\rho}{\mu}\right)^{0.8} (\text{Pr})^{1/3} \frac{u^{0.8}}{D'^{0.2}} \tag{56}$$

where u is defined by equation (49). Hence, the average coefficient in compartment 1 for Stream 1 is given by

$$h_l = \frac{1}{2b} \int_0^{2b} h_l' dx \tag{57}$$

or

$$h_l = \frac{\chi_l}{2b} \int_0^{2b} \frac{u^{0.8}}{D'^{0.2}} dx \tag{58}$$

where

$$\chi_l = 0.023 \cdot \text{k} \left(\frac{\kappa\rho}{\mu}\right)^{0.8} \text{Pr}^{1/3} \tag{59}$$

(c) Combined Coefficient. It is recognized that the number of tubes in contact with the streams varies as a function of x. This consideration leads us to introduce weighting factors η_c and η_l to the crossflow and longitudinal flow coefficients, respectively. The crossflow weighting factor η_c for Stream i is defined as the ratio of twice the mean streamline amplitude to the range of Stream i. Thus, for Stream 1

$$\eta_c = \frac{a_1 + a_2}{r_2 + a_2} \tag{60}$$

Similarly, for Stream 2

$$\eta_c = \frac{a_3 + a_4}{a_4 + r_4 - r_3 + a_3} \tag{61}$$

The foregoing definition is based on the heuristic reasoning that the crossflow path of a stream is construed to lie between the limits of its mean streamline in this model. Hence, it is consistent to assume the tube rows in the range of the mean streamline to be fully effective.

The longitudinal flow weighting factor η_l is defined as the ratio of the average height of the interface stream (y-direction) to the stream height. Thus, for Stream 1,

$$\eta_l = \frac{1}{3b} \int_0^{3b} \frac{(y_2 - y_1)dx}{r_2 + a_2} = \frac{r_2 - r_1}{r_2 + a_2} \tag{62}$$

Similarly, for Stream 2

$$\eta_l = \frac{1}{3b} \int_0^{3b} \frac{(y_4 - y_3)dx}{R - r_3 + a_3} = \frac{r_4 - r_3}{R - r_3 + a_3} \tag{63}$$

Finally, the total film coefficient h_{ij} (for Stream i, compartment j) is given by the weighted scalar sum of the longitudinal and crossflow components, i.e.,

$$h_{ij} = \eta_c h_c + \eta_l h_l \tag{64}$$

The concept of summing the longitudinal and crossflow coefficients to calculate the total coefficient has little analytical basis. However, this concept has achieved acceptance in the double segmental baffle design in the absence of a rigorous correlation. We retained it for the same reason.

In this manner the coefficient for each stream in each compartment is computed. The overall film coefficient for the baffle set is

$$h_s = \frac{2}{N}\left[N_1\left(\frac{2h_{11}}{3} + \frac{h_{12}}{3}\right) + N_2\left(\frac{h_{21}}{3} + \frac{2h_{22}}{3}\right)\right] \tag{65}$$

where N is the total number of tubes in the heat exchanger (equation (1)), and N_1 and N_2 are the number of tubes in the flow regimes of Streams 1 and 2, respectively. Thus

$$N_1 = \sum_{i=1}^{j^*} n_i \tag{66}$$

where j^* is given by

$$h_{j^*} < r_2 + a_2 < h_{j^*+1} \tag{67}$$

Similarly N_2 is given by

$$N_2 = \sum_{i^*}^{M} n_i \tag{68}$$

where i^* is given by the following inequality:

$$h_{i^*-1} < r_3 - a_3 < h_{i^*} \tag{69}$$

Equation (65) gives the overall coefficient by averaging the products of h_{ij} with their respective tube surface areas. h_s, given by equation (65), should be corrected for end zone effects, as described in Section 6.

5 Flow-Induced Vibration

The central variable instrumental in causing flow-induced vibration in liquid-to-liquid heat exchangers is the cross component of the flow velocity [1]. In Section 3, a method to determine the crossflow velocity at all tube rows (in the path of the mean streamline) was given. Having determined the crossflow velocity, any known prediction method [16] may be utilized to determine the vibration potential. Detailed formulae and guidelines are omitted here since they are available elsewhere in the literature [1, 18].

It is, however, important to point out that the window tubes which have three times the unsupported span of a typical overlap row tube of Stream 1 in compartment 2 may be the controlling row for design from vibration standpoint. The reason is that the tube natural frequency is approximately proportional to the square of unsupported span, and hence the required crossflow velocity to induce reasonant vibration in window tubes in quite small. Fortunately, the crossflow velocities in the window region are usually much smaller than those in the overlap region, as is apparent from the Piecewise Continuous Cosine Model.

In addition to the central spans, the end zones and inlet and outlet regions should also be studied for flow-induced vibration. Singh [16] has given a method to evaluate the vibration potential in the U-bend regions.

6 Discussion

A method to calculate shell side pressure drop ΔP for one baffle set and the stream ratio was given in Sections 2 and 3. To determine the total pressure drop in the shell stream, ΔP should be multiplied by the number of baffle sets. Furthermore, the pressure loss in the inlet and outlet nozzles (entrance and exit losses) should be added to the bundle loss to compute the overall pressure drop in the heat exchanger. Strictly speaking, the flow field in the end zones (for TEMA type E shells) cannot be modeled by streamlines, because of the abrupt stream mixings and flow direction changes that occur in the end zones. The end zones baffle spacings are also usually larger than the central spacing. The problem is further complicated by the arbitrariness of location and orientation of the nozzles. These effects are not yet quite understood. In view of these complexities, safety considerations warrant that we impose a blanket correction factor on the shell side film coefficient for the end zone region. It is recommended to define the shell side film coefficient for the end zones, $h_s{}^e$ by

$$h_s{}^e = \xi h_s \tag{70}$$

where

$$\xi = \text{Min}\left[\left(\frac{b}{b_e}\right)^2, 1\right] \tag{71}$$

where b_e is end zone baffle spacing.

Singh [16] has given a basis to determine the effective film coefficient for the U-bend regions under certain baffling conditions.

The end zone may be treated as identical to the central zones in medium length bundles for pressure drop calculations without significant error.

Finally, as we observed before, the Piecewise Continuous Cosine Model described in this paper gives the longitudinal and crossflow components of the flow velocity as a function of the tube row location. This enables computing the vibration susceptibility of each tube row. To the best of our knowledge, this is the first analytical flow model capable of producing a deterministic flow velocity profile for each tube row, including the window rows.

An enterprising heat exchanger designer has numerous parameters that he can vary to arrive at the most appropriate design. Tube size, layout pitch, layout angle, number of shell, and tube side passes, not to mention baffle type and baffle cuts, are various parameters that can be adjusted to "tune into" the proper design. Hence, the solution is obtained essentially by "trial and error." A variable often neglected in the optimization process is the relative open window areas in the three baffle types (Fig. 3). Setting window areas such that the window velocities at all baffle locations are as close to each other as possible is a desirable design goal. We have found that the total pressure drop can sometimes be reduced by as much as 10 percent without sacrificing heat transfer by adjusting the window areas. It should be noted that equal window areas do not produce equal flow velocities at all window locations, since the streams are not in strict longitudinal flow at all baffle windows. For example, Fig. 2 shows that the velocity vector of Stream 1 is not parallel to the x-axis at plane C (window of single slot baffle), although it is parallel to x-axis at planes A and D.

In critique, it must be stated that significant associated problems are still unsolved. Greater accuracy in the results will inevitably be derived from the development of an appropriate flow model for the end zones and evaluation of leakage and bypass substreams. Furthermore, the influence of shell curvature in distorting the planar flow profile (assumed in this paper) is still unknown. Admittedly, the shell curvature effect will be more pronounced in conventional baffle types (single segmental), yet its influence in triple segmental designs may not be insignificant. These problems, among others, must be solved to develop a complete understanding of baffled shell-and-tube fluid flow.

References

1 Nelms, H. A., and Segaser, C. L., "Survey of Nuclear Reactor System Primary Circuit Heat Exchangers," Oak Ridge National Laboratory Report No. ORNL-4399, Apr. 1969.

2 Kern, D. Q., *Process Heat Transfer*, McGraw-Hill, New York, 1950, pp. 129–130.

3 Mueller, A. C., *Handbook of Heat Transfer*, Rohsenow, W. M., and Hartnett, J. P., eds., Section 18, McGraw-Hill, New York, 1973, pp. 18–39.

4 "Design Guide for Heat Transfer Equipment in Water-Cooled Nuclear Reactor Systems," ORNL-TM-3578, pp. 165–201, Oak Ridge National Laboratory, Contract No. W-7405-eng-26, July 1975.

5 Tinker, T., "Shell Side Characteristics of Shell-and-Tube Heat Exchangers, A Simplified Rating System for Commercial Heat Exchangers," TRANS. ASME, Vol. 80, 1958, pp. 36–52.

6 Tinker, T., "Shell Side Characteristics of Shell and Tube Heat Exchangers," *General Discussion of Heat Transfer*, Institution of Mechanical Engineers and ASME, London, England, 1951, pp. 97–116.
gland, 1951, pp. 97–116.

7 Palen, J. W., and Taborek, J., "Solution of Shell Side Flow Pressure Drop and Heat Transfers by Stream Analysis Method," *Chemical Engineering Progress Symposium*, Vol. 65, No. 92, 1969, pp. 53–63.

8 Jacob, M., and Hawkins, G. A., *Elements of Heat Transfer*, 3rd ed., Wiley, New York, 1957, p. 122.

9 Taborek, J., "Design Methods to Heat Transfer Equipment—A Critical Survey of the State-of-the-Art," *Heat Exchangers: Design and Theory Sourcebook*, Afgan, N., and Schlünder, E. V., eds., Scripta Book Co., Washington, D. C., 1974, pp. 45–74.

10 Grimison, E. D., "Correlation and Utilization of New Data on Flow Resistance and Heat Transfer for Cross Flow of Gases over Tube Banks," TRANS. ASME, Vol. 59, 1937, pp. 583–594.

11 University of Delaware Engineering Experiment Station, Bulletin No. 2.

12 Žukauskas, A. A., "Heat Transfer of Banks of Tubes in Crossflow in High Reynolds Numbers," *Heat Exchangers: Design and Theory Sourcebook*, Afgan, N., and Schlünder, E. V., eds., Scripta Book Co., Washington, D. C., 1974, pp. 75–100.

13 "Flow in Rough Pipes," translation in NACA Tech. Mem., 1950.

14 "Friction Coefficients in Circular Tubes Having Square-Thread Roughness," NACA, 1952.

15 Carnahan, B., Luther, H. A., and Wilkes, D. O., *Applied Numerical Methods*, Wiley, New York, 1969, pp. 71–75.

16 Singh, K. P., "Predicting Flow Induced Vibration in U-bend Regions of Heat Exchangers—An Engineering Solution," to be published, *Journal of the Franklin Institute*.

17 Chenoweth, J. M., and Kistler, R. S., "Tube Vibrations in Shell and Tube Heat Exchangers," presented at the AIChE-ASME 15th National Heat Transfer Conference, San Francisco, Calif., Aug. 10–18, 1975.

18 Fitz-Hugh, J. H., "Flow Induced Vibation in Heat Exchangers," presented at International Symposium on Vibration Problems in Industry, Keswick, U. K., Apr. 10–12, 1973.

19 *Standards of Tubular Exchanger Manufacturers Association*, 5th ed., TEMA, Inc., New York, 1968.

20 Singh, K. P., "How to Locate Impingement Plates in Tubular Heat Exchangers," *Hydrocarbon Processing*, Oct. 1974, pp. 147–149.